

Oriental order on curved surfaces - the high temperature region

This article has been downloaded from IOPscience. Please scroll down to see the full text article.

2000 J. Phys. A: Math. Gen. 33 1139

(<http://iopscience.iop.org/0305-4470/33/6/304>)

View [the table of contents for this issue](#), or go to the [journal homepage](#) for more

Download details:

IP Address: 171.66.16.124

The article was downloaded on 02/06/2010 at 08:46

Please note that [terms and conditions apply](#).

Oriental order on curved surfaces—the high temperature region

Georg Foltin[†] and Raphael A Lehrer[‡]

[†] Institut für Theoretische Physik IV, Heinrich-Heine-Universität Düsseldorf,
Universitätsstrasse 1, D-40225 Düsseldorf, Germany

[‡] Lyman Laboratory of Physics, Harvard University, Cambridge, MA 02138, USA

Received 9 August 1999, in final form 6 December 1999

Abstract. We study orientational order, subject to thermal fluctuations, on a fixed curved surface. We derive, in particular, the average density of zeros of Gaussian distributed vector fields on a closed Riemannian manifold. Results are compared with the density of disclination charges obtained from a Coulomb gas model. Our model describes the disordered state of two-dimensional objects with orientational degrees of freedom, such as vector ordering in Langmuir monolayers and lipid bilayers above the hexatic to fluid transition.

1. Introduction

In several areas of statistical physics and condensed matter, a great deal of progress has been achieved by focusing on the physics of topological defects, ignoring other degrees of freedom. The Kosterlitz–Thouless transition, describing the destruction of orientational order in thin films, is a particularly important example. The transition is viewed as one where defect pairs unbind and proliferate, destroying the (quasi-) long-range order [1]. Another crucial example is that of type-II superconductors in a magnetic field, where the important physics is encoded in the properties of vortex lines (for a recent review, see [2]). Even in the absence of a magnetic field, the formation and growth of vortex loops can be used to explain the form of the voltage versus current relation [3]. Yet a third example is found in the physics of orientational order in membranes, where many workers [4–7] have found it fruitful to focus on the properties of topological defects to understand the low-temperature physics.

In all of these examples, topological defects are used primarily to understand the low-temperature behaviour. For example, in the case of superconductors, the vortex line description is used primarily to understand the behaviour below T_c (or H_{c2}), rather than to understand the properties of the normal metal phase at higher temperatures. Indeed, topological defects are a more natural description at low temperatures, where it is very costly to excite the order parameter away from its average value. Although themselves energetically costly, topological defects are the minimal-energy way of satisfying a constraint of the system, e.g., the curvature of a membrane or the penetration of a magnetic field into a superconductor.

At higher temperatures, the description becomes less natural. Order parameter fluctuations become much less costly, and hence the fluctuations observed in thermal equilibrium become more violent. At sufficiently high temperatures, the broken symmetry associated with the low-temperature phase is restored, and the average value of the order parameter is zero. Above this temperature, the order parameter behaves approximately like a Gaussian random variable.

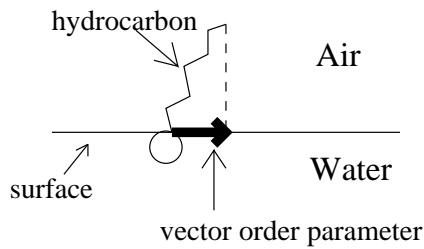


Figure 1. A surfactant molecule tilted away from the normal.

In this case, it seems that the description in terms of topological defects will be insufficient to describe the physics, as it only encodes the locations (and signs) of the zeros of the order parameter, classifying as irrelevant any fluctuations that the order parameter undergoes between these zeros.

Despite these objections, a description in terms of topological defects actually approximates the high-temperature behaviour of such systems quite well. For the case of thin films, Halperin [8] showed that the density of topological defects (i.e. zeros of the order parameter) that one obtains from a Gaussian order parameter are much the same as those from a Coulomb gas model that allows only the topological defects as degrees of freedom. In the case of superconductors, Lehrer and Nelson [9] have shown that above H_{c2} , a Gaussian approximation to the Ginzburg–Landau free energy predicts approximately the same distribution of vortex loops and lines as does the London theory, which is purely a description in terms of topological defects.

In this paper, we focus on the case of membranes. In particular, we examine the density of topological defects under the approximation that the free energy is Gaussian. This approximation will be valid at high temperatures. We compare these results to those obtained from a model which focuses *only* on the topological defects and their interactions, namely, a Debye–Hückel approximation to a Coulomb gas model.

One way to probe the high-temperature properties of a topologically spherical surface is with light scattering experiments on lipid vesicles [10]. In the case of lipid bilayers, the source of the orientational order parameter is the vector between a lipid head and a neighbouring head, and the order parameter describes the tendency of the lipids to achieve hexatic order at low temperatures. (The hexatic order and the transition to the disordered phase were studied in freestanding liquid-crystal films using light and x-ray scattering [11].) However, since this order parameter is invariant under rotations by 60° (because most lipids have six neighbours on average), it is slightly different from the case we consider, where the order parameter is only invariant under rotation by integer multiples of 360° . Nevertheless, we expect much of what we derive here to apply to these systems.

A system that is closer to what we consider here is that of tilted Langmuir monolayers (for a recent review, see [12]), which consist of a monolayer of lipids or amphiphiles on a liquid surface, e.g. the surface of a water droplet. The surfactant molecules have a tendency to orient themselves so that the hydrocarbon chain is tilted away from the normal to the surface. The projection of the direction of the polymer chain onto the surface forms an orientational order parameter which is exactly of the form that we consider in this paper, as illustrated in figure 1. A similar situation may be obtained in a lipid bilayer when the lipids tend to tilt away from the normal to the surface [13, 14], providing yet another source for an orientational order parameter.

The rest of the paper is organized as follows. In section 2, we write down a continuum model for the orientational order parameter that has the correct symmetries and should describe

both the low- and the high-temperature physics of the orientational order parameter, namely, an $O(2)$ Ginzburg–Landau theory in curved space. From this, we will derive a Coulomb gas model, and use it to calculate the density of disclination defects in the Debye–Hückel approximation in the high-temperature limit. We obtain

$$2\pi\rho = K + \frac{1}{4\pi^2 K_A x} \Delta K + O(x^{-2}) \quad (1.1)$$

where ρ is the density of defects, K is the curvature of the surface, Δ is the Laplace–Beltrami operator, x is the fugacity of the topological defects, and K_A describes the interaction strength of the defects.

In section 3, we present the main results of our paper. We approximate our model by neglecting the nonlinear terms, valid at high temperatures, and calculate the density of defects for an arbitrarily curved surface. For simplicity, we restrict our scope to closed surfaces—namely surfaces that are topologically equivalent to spheres, tori, etc. We especially focus on the case where the surface is topologically equivalent to a sphere, both for calculational ease and because we expect this class of (closed) surfaces to be the most easily amenable to experiments. Because the calculation is fairly technical, we first review Halperin’s calculation of the density of topological defects that we expect to see in flat space as a ‘toy model’ for the problem in curved space. We then proceed to the calculation in curved space, obtaining

$$2\pi\rho = K + \frac{\Delta K}{12\pi Z\tau} + O(\tau^{-2}) \quad (1.2)$$

where τ measures the deviation from the critical temperature, $Z^{-1} = 2\pi/\log(1/(a^2\tau))$, and a is a short-distance cutoff. Instead of using a gauge-field representation of the orientational order parameter we deal with a manifestly gauge-invariant picture. Employing a special symmetry of the model we can express the director field through simple scalar fields and solve it exactly in a high-temperature expansion.

The result for the defect density in curved space is equivalent to the Coulomb-gas/Debye–Hückel result above, provided we identify $\pi K_A x = 3Z\tau$. This confirms the validity of the Coulomb model even for high temperatures at this level of approximation. Deviations do, however, begin to show up at $O(\tau^{-2})$, as we shall show below.

2. Model and Debye–Hückel theory

We concentrate on the case of purely in-plane orientational order and therefore use a (two-component) tangential vector field $u_i(\sigma)$ as the order parameter. To describe the physics of the surface, we rely on the language of Riemannian differential geometry, which ensures that results are independent of any particular coordinate system. (A concise introduction to differential geometry of surfaces can be found in [15].) The order parameter lives on a closed two-dimensional Riemannian manifold with line element $ds^2 = g_{ij} d\sigma^i d\sigma^j$, where $g_{ij} = g_{ij}(\sigma^1, \sigma^2)$ is the metric tensor and $\sigma = (\sigma^1, \sigma^2)$ are internal coordinates of the surface. Using this formalism, we write down an $O(2)$ -invariant, statistical weight $P[u] \propto \exp(-H/T)$ for the u_i -field, where H is the (mesoscopic) Hamiltonian and T is the temperature. The simplest such Hamiltonian H is the analogue of Ginzburg–Landau theory in flat space, namely

$$\frac{H}{T} = \frac{1}{2} \int dA (D_i u_j D^i u^j + \tau u_i u^i + c(u_i u^i)^2) \quad (2.1)$$

where $dA = \sqrt{g}(\sigma) d\sigma^1 d\sigma^2$ is the invariant area element, g is the determinant of the metric, D_i is the covariant gradient, $u^i = g^{ij} u_j$, $g^{ij} = (g^{-1})_{ij}$, c is the coupling constant, and the coupling constant for the gradient term is absorbed into the field u_i . Equation (2.1) encodes

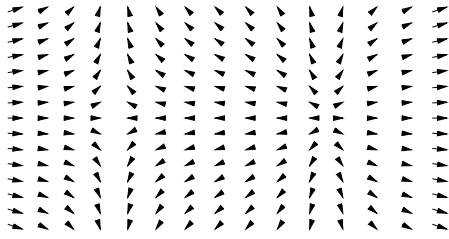


Figure 2. The planar vector field $(u_x, u_y) = (x^2 - 1, y)$ with a negative zero (left) and a positive zero (right).

the same physics as the free energy used by Park *et al* [5] and by Evans [6] for vector defects, although theirs appears in the gauge-field picture. The equivalence of the models is shown explicitly in appendix C.

For τ below a certain critical τ , this will be a ‘Mexican hat potential’; however, we will be concerned primarily with the opposite case, that of high temperatures ($\tau \gg 0$). Before we specialize to this case, we look at some properties at smaller τ . A critical temperature τ_c (the mean field value $\tau_c = 0$ gets renormalized due to fluctuations) separates the disordered state $\tau > \tau_c$ (high-temperature region) from the ‘ordered state’ $\tau < \tau_c$. We put ‘ordered state’ in quotation marks, because a perfectly ordered state is impossible for certain manifold topologies. For example, on a sphere or any other surface with the same topology, a tangential vector field has at least two zeros (defects) [15]. This can be illustrated by attempting to comb a hedgehog or a hairy ball: there will be two places where the vector field is zero or has a singularity.

To investigate this in more detail, we distinguish between two types of zeros. One type, called a ‘positive zero’, is characterized by $\det(D_i u_j) > 0$, while the other type, a ‘negative zero’, has a saddle-like flow and is characterized by $\det(D_i u_j) < 0$. See figure 2 for an illustration of these types of defects. Zeros with $\det(D_i u_j) = 0$ do not fall into this scheme; however, they will not show up in a statistical model as the probability to hit exactly $\det(D_i u_j) = 0$ vanishes. The number of positive zeros minus the number of negative zeros is a topological constraint and equal to $2(1 - \gamma)$, where γ is the number of handles of the (closed) surface, e.g. zero for a spherical topology and one for a torus [15]. We will show this theorem explicitly en route to our calculation. Thus, on surfaces other than tori, the low-temperature phase necessarily has defects, unlike in flat space, where the ground state is defect free.

As in flat space, the properties of the low-temperature phase are determined by low-energy Goldstone modes (‘spin waves’), which prevent true long-ranged correlations. Instead, one finds an algebraic decay of the correlations (quasi-long-ranged order). Besides the spin waves, thermally excited defects persist. Integration over the spin waves results in a Coulomb gas model for these defects (zeros) [7], where the defects carry a charge proportional to their index $q = \text{sign} \det(D_i u_j)$ and a core energy (chemical potential [16]). The interaction energy of the defects reads

$$\frac{H}{T} = \frac{K_A}{2} \int dA \int dA' (2\pi\rho - K)_\sigma G(\sigma, \sigma') (2\pi\rho - K)_{\sigma'} \quad (2.2)$$

where $G(\sigma, \sigma')$ denotes the Green function of the negative of the Laplace–Beltrami operator $-\Delta = -g^{ij} D_i \partial_j$ † and K_A is the coarse-grained effective coupling between the defects and therefore depends on the temperature [1, 17]. ρ is the defect density $\rho(\sigma) = \sum_i q_i \delta_c(\sigma, \sigma_i)$,

† The Green function of the negative of the Laplace–Beltrami operator Δ is the ‘electrostatic’ potential at the point σ of a unit charge located at point σ' and of a negative unit charge which is uniformly distributed over the surface to ensure charge neutrality. It is given by $-\Delta G(\sigma, \sigma') = \delta_c(\sigma, \sigma') - 1/A$, where δ_c is the covariant delta function and A is the area of the surface.

where σ_i are the locations of the defects and δ_c is the covariant version of the Dirac delta function given by

$$\delta_c(\sigma, \sigma') = \lim_{\lambda \rightarrow \infty} \frac{\lambda}{2\pi} \exp\left(-\frac{\lambda}{2} d^2(\sigma, \sigma')\right) = \delta^2(\sigma - \sigma') / \sqrt{g}(\sigma)$$

($d(\sigma, \sigma')$ is the geodesic distance between σ and σ'). We note that the Gaussian curvature $K = K(\sigma)$ plays the role of a background charge density. Because of this, positive defects tend to concentrate in regions with positive curvature, whereas negative defects prefer saddle-shaped regions with negative curvature. Charge neutrality and the Gauss–Bonnet theorem [15] $2\pi \sum_i q_i - \int dA K = 0$ yield the topological constraint $\sum_i q_i = 2(1 - \gamma)$.

Above a certain temperature it is expected [7] that the low-temperature phase with a few tightly bound defects is destroyed through unbinding of defect pairs, analogous to the Kosterlitz–Thouless transition in flat space. The high-temperature phase has a finite density of thermally excited, unbound defects. The interaction between the defects is screened, with a screening length of the order of the typical distance of the defects (Debye–Hückel length). Above the transition temperature, we make a Gaussian approximation of the Coulomb gas model (2.2) with a *continuous* defect density ρ

$$\frac{H}{T} = \frac{K_A}{2} \int dA \int dA' (2\pi\rho - K)_\sigma G(\sigma, \sigma') (2\pi\rho - K)_{\sigma'} + \frac{1}{2x} \int dA \rho^2 \tag{2.3}$$

where x is the fugacity of the charges. By setting $\delta H / \delta \rho = 0$, we obtain for the mean charge density

$$2\pi\rho = \frac{1}{1 - \frac{1}{4\pi^2 K_A x} \Delta} K = K + \frac{1}{4\pi^2 K_A x} \Delta K + O(x^{-2}). \tag{2.4}$$

Although this approximation accurately represents the Coulomb gas at high temperatures, the use of the Coulomb gas at all to describe the high-temperature phase is rather suspect. Nevertheless, we show that the Coulomb gas model yields a density of defects which agrees remarkably well with the density obtained from (2.1) in the high-temperature phase on an arbitrary curved surface.

3. Charge density in the high-temperature Gaussian approximation

In the remainder of the paper we present the calculation of the defect density ρ from (2.1) in the disordered state, where the quartic term $\int dA (u_i u^i)^2$ is irrelevant and can be neglected. We expect that similar to the situation in curved space–time [18], a term proportional to $\int dA K u_i u^i$ is generated under renormalization, where $K = K(\sigma)$ is the Gaussian curvature. Since K has the dimension of $1/\text{length}^2$ this term is as relevant as the gradient term. Thus, in the high-temperature phase the vector field is distributed according to the Gaussian weight

$$P[u] \propto \exp\left(-\frac{1}{2} \int d^2\sigma \sqrt{g} (D_i u_j D^i u^j + \tau u^i(\sigma) u_i(\sigma) + \eta K u^i u_i)\right) \tag{3.1}$$

where τ is now the mass of the vector field and η is the coupling of K to $u_i u^i$. In addition, the distribution for u_i has to be equipped with a covariant cutoff procedure, such as the heat kernel regularization [19]. Because the model depends only on the intrinsic geometry of the manifold, no extrinsic couplings (such as a term proportional to $C^2 u_i u^i$, where C is the mean curvature of the surface) can be generated under renormalization.

The zeros of the field u_i are characterized by the index $q = \text{sign det}(D_i u_j) = \pm 1$. The index (charge) describes the local topology of a flow u_i near a zero $u_i(\sigma) = 0$. The corresponding mean charge density is given by

$$\rho(\sigma) = \left\langle \sum_i q_i \delta_c(\sigma, \sigma_i) \right\rangle \quad (3.2)$$

where the defects are labelled by the index i , located at coordinates σ_i , and have charges q_i . The expectation value is taken with respect to the probability distribution of (3.1).

Transforming from the variable σ to the variable u via the Jacobian, we obtain

$$\rho = \langle \det(D_i u^j(\sigma)) \delta_c(u(\sigma)) \rangle \quad (3.3)$$

which can be seen easily using a locally Euclidean coordinate system and linearizing the vector field around the zero $u_j(x_1, x_2) = x_k \alpha_{kj}$:

$$\begin{aligned} & \int d^2x \det(\partial_i(x_k \alpha_{kj})) \delta^2(x_k \alpha_{kj}) \\ &= \int d^2x |\det(\alpha_{ij})| \text{sign det}(\alpha_{ij}) \delta^2(x_k \alpha_{kj}) = \text{sign det}(\alpha_{ij}) = \pm 1. \end{aligned} \quad (3.4)$$

To calculate the expectation value (at point σ) $\rho(\sigma)$ one needs the joint distribution of $u_i(\sigma)$ and $D_i u_j(\sigma)$ which can be determined since $u_i(\sigma)$ and $D_i u_j(\sigma)$ are a set of (multicomponent) Gaussian random variables with correlations $\langle u_i(\sigma) u_j(\sigma) \rangle$, $\langle u_k(\sigma) D_i u_j(\sigma) \rangle$, $\langle D_i u_j(\sigma) D_k u_l(\sigma) \rangle$.

3.1. Density of defects in flat space

Before calculating results in curved space, we review Halperin's calculation for the density of zeros of a Gaussian two-component order parameter u in two-dimensional flat space [8]. Equation (3.1) becomes

$$P[\mathbf{u}(\mathbf{r})] \propto \exp \left\{ -\frac{1}{2} \int d^2r [(\partial_i u_j)^2 + \tau u^2] \right\} \quad (3.5)$$

and (3.3) becomes

$$\rho(\mathbf{r}) = \langle \delta^2[\mathbf{u}(\mathbf{r})] \det(\partial_i u_j) \rangle. \quad (3.6)$$

This expectation value is completely determined by the probability distribution $P(\xi_i, \alpha_{ij})$, where $\xi_i = u_i(\mathbf{r})$ and $\alpha_{ij} = \partial_i u_j(\mathbf{r})$ via the formula

$$\rho(\mathbf{r}) = \int d^4 \alpha_{ij} P(\mathbf{0}, \alpha_{ij}) \det \alpha_{ij}. \quad (3.7)$$

Since (3.5) is Gaussian, this probability distribution is just given by

$$P(\xi_i, \alpha_{ij}) = \frac{1}{(2\pi)^3} \frac{1}{[\det M_{ij}]^{1/2}} \exp \left\{ -\frac{1}{2} x_i M_{ij}^{-1} x_j \right\} \quad (3.8)$$

where x is a six-component vector given by $x = (\xi_1, \xi_2, \alpha_{11}, \alpha_{12}, \alpha_{21}, \alpha_{22})$, and M_{ij} is the matrix of correlations $M_{ij} = \langle x_i x_j \rangle$. Plugging (3.8) into (3.7) gives

$$\rho = \frac{1}{2\pi} \left(\frac{\det \tilde{M}_{ij}}{\det M_{ij}} \right)^{1/2} (\tilde{M}_{14} - \tilde{M}_{23}) \quad (3.9)$$

where \tilde{M} is the matrix of correlations $M_{ij} = \langle y_i y_j \rangle$, and y is a four-component vector given by $(\alpha_{11}, \alpha_{12}, \alpha_{21}, \alpha_{22})$.

The expectation values necessary to evaluate (3.9) can be readily determined from (3.5). The result is that $\rho(\mathbf{r}) = 0$, as expected by symmetry: the system is uniform and charge-neutral. In order to obtain a nontrivial result to compare with the Coulomb gas model, we must calculate the correlation function of the density of charges, defined by

$$C(\mathbf{r}) = \langle \rho(\mathbf{r})\rho(\mathbf{0}) \rangle = \langle \delta^2[\mathbf{u}(\mathbf{r})] \det[\partial_i u_j(\mathbf{r})] \delta^2[\mathbf{u}(\mathbf{0})] \det[\partial_i u_j(\mathbf{0})] \rangle. \quad (3.10)$$

This can be evaluated by similar methods, and the results match up very well with the Coulomb gas model [8].

3.2. Density of defects in curved space

In the case of a general closed membrane, ρ will already be nontrivial for two reasons. First, the system is not charge-neutral, but rather the total charge must be equal to 2 minus the number of handles on the surface (e.g. 2 for a sphere, zero for a torus, etc). Second, unless the surface has a high degree of symmetry, the charge will not distribute itself uniformly. Rather, the charge density will depend upon the local curvature of the surface. Thus, for the case we consider in the remainder of the paper, we can get a meaningful comparison with the Coulomb gas theory solely from calculating the charge density ρ , rather than needing to calculate the more complicated correlation functions.

The method used is conceptually the same as in section 3.1, but more technically complicated due to the curvature of the space. Therefore, we present it in appendix A. The analogous result to (3.9) for a *general* Gaussian, $O(2)$ invariant distribution for the vector field u_i is

$$2\pi\rho - K = \epsilon^{ik}\epsilon^{jl}D_k \left(\frac{\langle (D_i u_j) u_l \rangle}{\langle u_m u^m \rangle} \right). \quad (3.11)$$

Since the right-hand side of (3.11) is a total divergence, we find, after integration over the surface the aforementioned topological constraint for the total charge of the defects

$$2\pi \int dA \rho = \int dA K = 4\pi(1 - \gamma) \quad (3.12)$$

which agrees with the Gauss–Bonnet theorem, as $1 - \gamma$ is the genus of the surface.

To derive ρ from (3.11), we need to calculate $\langle u_i u_j \rangle$ and $\langle (D_i u_j) u_k \rangle$. This can be done in an expansion with respect to the interaction range $1/\tau$ using the Gaussian weight (3.1). It is convenient to decompose the vector field u_i into a sum of a gradient and a curl, $u_i = \partial_i \phi + \epsilon_i^j \partial_j \chi$. This representation is only valid for (deformed) spheres. For other topologies, modes exist which cannot be written as a sum of a gradient and a curl. For example, in a torus, a vector field that represents a flow along one of the perimeters cannot be decomposed in this way.

A particularly simple case is given for $\eta = 1$ because the potentials ϕ and χ decouple. The special role of the $\eta = 1$ case can also be understood within the gauge-field representation, as shown in appendix D. For this case, we derive the density of defects in a high-temperature expansion. For high temperatures, the screening length is small compared with the radius of curvature: the surface appears to be almost flat. Upon increasing screening length, more details of the geometry become relevant. We present the details of this high-temperature expansion in appendix B, obtaining as our main result the average defect density ρ :

$$2\pi\rho = K + \frac{\Delta K}{12Z\pi\tau} + \frac{\Delta^2 K}{120Z\pi\tau^2} - \frac{\Delta K^2}{30Z\pi\tau^2} + O(\tau^{-3}) \quad (3.13)$$

where $Z^{-1} = 2\pi / \log(1/(a^2\tau))$, and a is a short-distance cutoff.

To lowest order in the correlation length $\tau^{-1/2}$, this is equivalent to the Debye–Hückel approximation (2.4) provided one identifies $\pi K_A x = 3Z\tau$. For larger correlation lengths, however, deviations show up. The term $\propto \tau^{-1}$ will be independent of the coupling η for dimensional reasons. The next orders, however, depend on η . We conjecture, that expansion (3.13) remains valid for arbitrary genus of the surface. Treating general genus and η , however, requires the calculation of moments of the vector field u_i directly, which is much more complicated and beyond the scope of this work.

It will be difficult to observe the defect density (3.13) experimentally, since ρ , which is the density of positive defects *minus* the density of negative defects is of the order of $\rho \sim 1/A$ due to the topological constraint (3.12). On the other hand, the density of positive defects plus the density of negative defects is of the order of $1/\xi^2 \sim \tau$, where ξ is the correlation length, which is small well above the transition temperature. In the high-temperature phase, therefore, we have to measure a tiny density difference in the presence of a large background density. Closer to the transition region the background density becomes smaller and there might well be a chance to resolve the defects in thin films using polarized light. It would certainly be interesting to see whether our expansion (3.13) or the result (2.4) obtained from the Coulomb gas model allow for a better fit to the experimental data.

4. Conclusion

We have derived the average topological charge density of vector fields with a Gaussian distribution on a curved surface. We found that for high temperatures, the zeros behave like (screened) charges in the presence of a background charge density equal to the Gaussian curvature. We demonstrated the validity of the Debye–Hückel approximation of the Coulomb gas model, which, as discussed in section 1, is not obvious, since the Coulomb gas model originates from a low-temperature model of the orientational order and we are attempting to apply it in a high-temperature regime.

Acknowledgments

We have benefited from discussions with DR Nelson and B I Halperin. GF was supported by the Deutsche Forschungsgemeinschaft through Grant Fo 259/1 and acknowledges the hospitality of the Condensed Matter Theory group at Harvard University, where some of this work was done. RAL was supported primarily by the Harvard Materials Research Science and Engineering Laboratory through Grant No DMR94-00396, by the National Science Foundation through Grant No DMR97-14725, and by the Office of Naval Research.

Appendix A. Calculation of charge density

We will calculate the density of defects $\rho = \langle \det(D_i u^j(\sigma)) \delta_c(u(\sigma)) \rangle$. We begin by exact analogy with the calculation for flat space outlined in section 3.1, by noting that this expectation value is completely determined by the probability distribution $P(v_i, A_{ij})$, where $v_i = u_i(\sigma)$ and $A_{ij} = D_i u_j(\sigma)$ via the formula

$$\rho(\sigma) = \int d^4 A_{ij} P(\mathbf{0}, A_{ij}) \det A_i^j. \quad (\text{A.1})$$

Since (3.1) is Gaussian, this probability distribution is just given by

$$P(v_i, A_{ij}) = \frac{1}{(2\pi)^3} \frac{1}{[\det M_{ij}]^{1/2}} \exp \left\{ -\frac{1}{2} x_i (M^{-1})^{ij} x_j \right\} \quad (\text{A.2})$$

where x_i is a six-component vector given by $(v_1, v_2, A_{11}, A_{12}, A_{21}, A_{22})$, and M_{ij} is the matrix of correlations $M_{ij} = \langle x_i x_j \rangle$.

We can re-express this as

$$P(v_i, A_{ij}) = \frac{1}{(2\pi)^6} \int d^4 \tilde{A}^{ij} \int d^2 \tilde{v}^i \exp \left\{ -\frac{1}{2} \tilde{x}^i M_{ij} \tilde{x}^j + i \tilde{x}^i x_i \right\} \quad (\text{A.3})$$

where \tilde{x}^i is a six-component vector given by $(\tilde{v}^1, \tilde{v}^2, \tilde{A}^{11}, \tilde{A}^{12}, \tilde{A}^{21}, \tilde{A}^{22})$. Performing the integral over the \tilde{x}^i returns us to (A.2). Explicitly, we have for the defect density

$$\begin{aligned} \rho = & \frac{1}{(2\pi)^6} \int d^4 \tilde{A}^{ij} d^4 A_{ij} d^2 \tilde{v}^i d^2 v_i \exp \left(-\frac{1}{2} \tilde{A}^{ij} \tilde{A}^{kl} \langle (D_i u_j)(D_k u_l) \rangle \right) \\ & \times \exp(-\tilde{A}^{ij} \tilde{v}^k \langle (D_i u_j) u_k \rangle - \frac{1}{2} \tilde{v}^i \tilde{v}^j \langle u_i u_j \rangle + i \tilde{A}^{ij} A_{ij} + i \tilde{v}^i v_i) \\ & \times \frac{1}{2} \epsilon^{ik} \epsilon^{jl} A_{ij} A_{kl} \delta_c(v). \end{aligned} \quad (\text{A.4})$$

The integration over the v_i yields a factor of \sqrt{g} since

$$\delta_c(v(\sigma)) = \lim_{\lambda \rightarrow \infty} \frac{\lambda}{2\pi} \exp \left(-\frac{\lambda}{2} g^{ij}(\sigma) v_i v_j \right) = \sqrt{g}(\sigma) \delta^2(v).$$

The resulting expression can be simplified by using the O(2)-invariance of the field u_i by noting that g_{ij} is the only rank-2 tensor invariant under O(2), and therefore

$$\langle u_i u_j \rangle = \frac{1}{2} g_{ij} \langle u_m u^m \rangle. \quad (\text{A.5})$$

After integration over the \tilde{v}^i we obtain

$$\rho = \frac{1}{2\pi \langle u_m u^m \rangle} \frac{1}{(2\pi)^4} \int d^4 \tilde{A}^{ij} d^4 A_{ij} \exp \left(-\frac{1}{2} \tilde{A}^{ij} \tilde{A}^{kl} T_{ijkl} + i \tilde{A}^{ij} A_{ij} \right) \epsilon^{ik} \epsilon^{jl} A_{ij} A_{kl} \quad (\text{A.6})$$

where

$$T_{ijkl} = \langle (D_i u_j)(D_k u_l) \rangle - 2 \frac{\langle (D_i u_j) u_m \rangle \langle (D_k u_l) u^m \rangle}{\langle u_n u^n \rangle}. \quad (\text{A.7})$$

Integrating over the \tilde{A}^{ij} in (A.6), we see that the A_{ij} are simply Gaussian variables with correlations given by

$$\langle A_{ij} A_{kl} \rangle = T_{ijkl}. \quad (\text{A.8})$$

Therefore, (A.6) yields

$$\rho = \frac{\epsilon^{ik} \epsilon^{jl} T_{ijkl}}{2\pi \langle u_m u^m \rangle}. \quad (\text{A.9})$$

To further simplify this equation, we derive

$$\begin{aligned} \epsilon^{ik} \epsilon^{jl} D_k \left(\frac{\langle (D_i u_j) u_l \rangle}{\langle u_m u^m \rangle} \right) &= \epsilon^{ik} \epsilon^{jl} \frac{\langle (D_k D_i u_j) u_l \rangle}{\langle u_m u^m \rangle} + \epsilon^{ik} \epsilon^{jl} \frac{\langle (D_i u_j)(D_k u_l) \rangle}{\langle u_m u^m \rangle} \\ &\quad - 2 \epsilon^{ik} \epsilon^{jl} \frac{\langle (D_i u_j) u_l \rangle \langle (D_k u_m) u^m \rangle}{\langle u_n u^n \rangle^2} \\ &= -K + \epsilon^{ik} \epsilon^{jl} \frac{T_{ijkl}}{\langle u_m u^m \rangle} \end{aligned} \quad (\text{A.10})$$

using the fact that in two dimensions, the Riemann curvature tensor is $R_{ijkl} = \epsilon_{ij} \epsilon_{kl} K$, (where K is the Gaussian curvature), and also that due to the O(2)-invariance of u_i ,

$$\langle (D_i u_j) u_k \rangle = \frac{1}{2} g_{jk} \langle (D_i u_m) u^m \rangle + \frac{1}{2} \epsilon_{jk} \epsilon^{mn} \langle (D_i u_m) u_n \rangle. \quad (\text{A.11})$$

We therefore arrive at an expression for the mean defect density

$$2\pi\rho - K = \epsilon^{ik} \epsilon^{jl} D_k \left(\frac{\langle (D_i u_j) u_l \rangle}{\langle u_m u^m \rangle} \right) \quad (\text{A.12})$$

valid for any Gaussian, O(2)-invariant distribution for the vector fields u_i .

Appendix B. High-temperature expansion

In this appendix, we derive the density of defects in a high-temperature expansion for the case $\eta = 1$, as discussed in section 3.2. In this case, since $D^i D_i \partial_j \phi - K \partial_j \phi = \partial_j \Delta \phi$, the eigenfunctions of the operator $-D_i D^i + K + \tau$ (acting on vector fields)

$$(-D^i D_i + K + \tau)u_{j,\alpha} = (\lambda_\alpha + \tau)u_{j,\alpha} \quad (\text{B.1})$$

can be written as $u_{i,\alpha}^{(1)} = \partial_i \phi_\alpha$ and $u_{i,\alpha}^{(2)} = \epsilon_i^j \partial_j \phi_\alpha$, where ϕ_α is a normalized eigenfunction of the Laplace–Beltrami operator $-\Delta \phi_\alpha = -g^{ij} D_i \partial_j \phi_\alpha = \lambda_\alpha \phi_\alpha$. Together with the normalization of the u_α

$$\int dA u_{j,\alpha} u^{j,\alpha} = \int dA g^{ij} \partial_i \phi_\alpha \partial_j \phi_\alpha = \lambda_\alpha$$

we obtain the propagator for u_i

$$\langle u_i(\sigma) u_j(\sigma') \rangle = \langle \partial_i \phi(\sigma) \partial_j \phi(\sigma') \rangle + \epsilon_i^k(\sigma) \epsilon_j^l(\sigma') \langle \partial_k \phi(\sigma) \partial_l \phi(\sigma') \rangle \quad (\text{B.2})$$

in terms of the *scalar* propagator

$$\langle \phi(\sigma) \phi(\sigma') \rangle = \sum'_\alpha \frac{\exp(-a^2 \lambda_\alpha)}{\lambda_\alpha (\lambda_\alpha + \tau)} \phi_\alpha(\sigma) \phi_\alpha(\sigma') \quad (\text{B.3})$$

where the zero mode $\phi \equiv \text{const}$ is omitted and a is an exponential cutoff length that arises from the heat kernel regularization. After some algebra we find

$$2\pi\rho - K = \epsilon^{ik} \epsilon^{jl} D_k \left(\frac{\langle (D_i \partial_j \phi) \partial_l \phi \rangle}{\langle \partial_m \phi \partial^m \phi \rangle} \right) = \frac{1}{2} D^k \left(\frac{\partial_k \langle \phi \Delta \phi \rangle - \partial_k \langle \partial_m \phi \partial^m \phi \rangle}{\langle \partial_n \phi \partial^n \phi \rangle} \right) \quad (\text{B.4})$$

with $\langle (\Delta \phi) \partial_i \phi \rangle = \frac{1}{2} \partial_i \langle (\Delta \phi) \phi \rangle$ from (B.3). Both $-\langle \phi \Delta \phi \rangle$ and $\langle \partial_m \phi \partial^m \phi \rangle$ are logarithmically divergent for small cutoff lengths

$$\left. \begin{array}{l} \langle \partial_m \phi \partial^m \phi \rangle \\ -\langle \phi \Delta \phi \rangle \end{array} \right\} = \frac{1}{4\pi} \log \left(\frac{1}{a^2 \tau} \right) + \text{finite parts}$$

where only the finite parts depend on the position on the manifold. Therefore the numerator of (B.4) is finite, whereas in the limit of small cutoff lengths the divergent denominator can be replaced by its most divergent (spatially constant) part. Defining $Z^{-1} = 2\pi / \log(1/(a^2 \tau))$, we obtain

$$2\pi\rho - K = Z^{-1} \Delta (\langle \phi \Delta \phi \rangle - \langle \partial_m \phi \partial^m \phi \rangle). \quad (\text{B.5})$$

Using $\langle \partial_m \phi \partial^m \phi \rangle = \frac{1}{2} \Delta \langle \phi^2 \rangle - \langle \phi \Delta \phi \rangle$ and $\tau \langle \phi^2 \rangle = \langle \phi \Delta \phi \rangle + \langle \phi(\tau - \Delta)\phi \rangle$, we obtain

$$2\pi\rho - K = Z^{-1} \left(\Delta \left(2 - \frac{1}{2\tau} \Delta \right) \langle \phi \Delta \phi \rangle - \frac{1}{2\tau} \Delta^2 \langle \phi(\tau - \Delta)\phi \rangle \right). \quad (\text{B.6})$$

The moment

$$\langle \phi(\tau - \Delta)\phi \rangle = \sum'_\alpha \frac{\exp(-a^2 \lambda_\alpha)}{\lambda_\alpha} \phi_\alpha(\sigma)^2$$

is the Green function of the Laplace–Beltrami operator at coinciding points, which can be obtained from conformal field theory. With the definition of the massless propagator and its short-distance behaviour $G(\sigma, \sigma') \sim \Gamma(\sigma) - \log(d(\sigma, \sigma'))/(2\pi)$, we find for two conformal equivalent metrics $g_{ij} = \zeta \tilde{g}_{ij}$ that $-\Delta \Gamma + 2/A - K/(2\pi) = (-\tilde{\Delta} \tilde{\Gamma} + 2/\tilde{A} - \tilde{K}/(2\pi))/\zeta$ and consequently for a spherical topology $-\Delta \Gamma = K/(2\pi) - 2/A$. A is the area of the surface and d the geodesic distance. We have $\Delta^2 \langle \phi(\tau - \Delta)\phi \rangle = -\Delta K/(2\pi)$. The moment $\langle \phi \Delta \phi \rangle$

has to be calculated in an asymptotic $1/\tau$ expansion. With the help of [19–21] we find for the finite part of $\langle \phi \Delta \phi \rangle$

$$-\langle \phi \Delta \phi \rangle = \frac{K}{12\pi\tau} + \frac{K^2 + \Delta K}{60\pi\tau^2} + \mathcal{O}(\tau^{-3}). \quad (\text{B.7})$$

Finally, we obtain the average defect density ρ

$$2\pi\rho = K + \frac{\Delta K}{12Z\pi\tau} + \frac{\Delta^2 K}{120Z\pi\tau^2} - \frac{\Delta K^2}{30Z\pi\tau^2} + \mathcal{O}(\tau^{-3}). \quad (\text{B.8})$$

Appendix C. The gauge-field representation

Orientational order is frequently represented as a gauge-field theory [5, 6]. The vector field u_i is represented in a local orthogonal base (reference frame) v_i by a complex function ψ through $u_i = v_i \text{Re}(\psi) + \epsilon_i^j v_j \text{Im}(\psi)$, where $v_i v^i = 1$ and ϵ is the antisymmetric unit tensor. Plugging this into (2.1), we obtain

$$\frac{H}{T} = \int d^2\sigma \sqrt{g} (g^{ij} (\partial_i \psi^* + i\Omega_i \psi^*) (\partial_j \psi - i\Omega_j \psi) + \tau |\psi|^2 + c |\psi|^4) \quad (\text{C.1})$$

with the vector potential $\Omega_i = \epsilon^{jk} v_j D_i v_k$, resulting from the fact that the reference frame v_i is changing from point to point. In this representation the Gaussian curvature K plays the role of a perpendicular magnetic field $\epsilon^{ij} D_i \Omega_j = K$. Since any unit vector field v_i must have two points on a sphere where it is singular, Ω_i will be singular at two points as well, even if the underlying surface is not. We therefore use (2.1) rather than (C.1) in this paper as a base for calculation. The disadvantage of (2.1) is that it is more difficult to generalize to an n -fold symmetry, as is done by Park *et al* [7] and Evans [6].

Appendix D. The $\eta = 1$ case

Equation (C.1) is covariant and gauge invariant, i.e. invariant against changes of the local frame v_i . For convenience, we choose a conformally flat coordinate system with a metric tensor $g_{ij} = \zeta(x, y) \delta_{ij}$, where the coordinates are $\sigma^1 \equiv x$, $\sigma^2 \equiv y$ and $\zeta(x, y)$ encodes the (intrinsic) geometry of the surface. A proof that such a coordinate system exists, as well as a review of its properties, can be found in [15]. (Note, however, that for closed surfaces other than tori, ζ will have singular points.) Furthermore, we choose a particular reference frame $v_x = \sqrt{\zeta}$, $v_y = 0$. Then $\sqrt{g} g^{ij} = \delta_{ij}$, $\Omega_x = \partial_y \omega$, $\Omega_y = -\partial_x \omega$, $K = (1/\zeta)(\partial_x^2 + \partial_y^2)\omega$ where $\omega = -\frac{1}{2} \log \zeta$. The Gaussian weight (3.1) becomes $P[\psi] = \exp(-\frac{1}{2} \int d^2x \psi^* \mathcal{H} \psi)$ with the Hamilton operator

$$\mathcal{H} = -(\partial_x - i\partial_y \omega)^2 - (\partial_y + i\partial_x \omega)^2 + \eta \nabla^2 \omega + \zeta \tau. \quad (\text{D.1})$$

For $\eta = 1$ and a vanishing mass $\tau = 0$ we can express the Hamilton operator in terms of the square of a Dirac-type operator ($\hat{\sigma}_{x,y,z}$ are the Pauli matrices)

$$\mathcal{H} = -[(\partial_x - i\partial_y \omega) \hat{\sigma}_x + (\partial_y + i\partial_x \omega) \hat{\sigma}_y]^2 = -(\partial_x - i\partial_y \omega)^2 - (\partial_y + i\partial_x \omega)^2 + \hat{\sigma}_z \nabla^2 \omega \quad (\text{D.2})$$

in the $\sigma_z = +1$ sector. The latter operator is the Hamiltonian of the 2D Pauli equation for spin- $\frac{1}{2}$ particles with the (dimensionless) magnetic moment $g = 2$ (electrons!) in a magnetic field $B_z = \nabla^2 \omega$. Thus the $\eta = 1$ case that we focus on is closely related to both the Dirac equation and the Pauli equation in two dimensions. The Dirac equation and its discretized counterpart are commonly used to describe the properties of electrons confined to a plane in a quenched, perpendicular magnetic field [22].

References

- [1] Kosterlitz J M and Thouless D J 1972 *J. Phys. C: Solid State Phys.* **5** L125–6
Kosterlitz J M and Thouless D J 1973 *J. Phys. C: Solid State Phys.* **6** 1181–203
- [2] Blatter G, Feigel'man M V, Geshkenbein V B, Larkin A I and Vinokur V M 1994 *Rev. Mod. Phys.* **66** 1125–388
- [3] Langer J S and Fisher M E 1967 *Phys. Rev. Lett.* **19** 560–3
Huse D A, Fisher M P A and Fisher D S 1992 *Nature* **358** 553
- [4] Ovrum B A and Thomas S 1991 *Phys. Rev. D* **43** 1314–22
- [5] Park J, Lubensky T C and MacKintosh F C 1992 *Europhys. Lett.* **20** 279–84
- [6] Evans R M L 1996 *Phys. Rev. E* **53** 935–49
- [7] Park J M and Lubensky T C 1996 *Phys. Rev. E* **53** 2648–64
- [8] Halperin B I 1981 *Physics of Defects* ed R Balian *et al* (New York: North-Holland) pp 813–57
- [9] Lehrer R A and Nelson D R Vortex fluctuations above H_{c2} , unpublished
- [10] Sackmann E 1995 *Structure and Dynamics of Membranes* vol 1A, ed R Lipowsky and E Sackmann (Amsterdam: Elsevier) pp 213–304
- [11] Brock J D, Aharony A, Birgeneau R J, Evans-Lutterodt K W, Litster J D, Horn P M and Stephenson G B 1986 *Phys. Rev. Lett.* **57** 98–101
Spector M S and Litster J D 1995 *Phys. Rev. E* **51** 4698–703
- [12] Kaganer V M, Möhwald H and Dutta P 1999 *Rev. Mod. Phys.* **71** 779–819
- [13] de Gennes P G and Prost J 1993 *The Physics of Liquid Crystals* 2nd edn (New York: Oxford University Press)
- [14] Chiang H-T, Chen-White V S, Pindak R and Seul M 1995 *J. Physique II* **5** 835–57 and references therein
- [15] David F 1989 *Statistical Mechanics of Membranes and Surfaces* vol 5, ed D R Nelson *et al* (Singapore: World Scientific) pp 157–223
- [16] Deem M W and Nelson D R 1996 *Phys. Rev. E* **53** 2551–9
- [17] Nelson D R and Peliti L 1987 *J. Physique* **48** 1085–92
- [18] Buchbinder I L, Odintsov S D and Lichtzier I M 1989 *Theor. Math. Phys.* **79** 558–62
Odintsov S D 1991 *Fortschr. Phys.* **39** 621–41
Buchbinder I L, Odintsov S D and Shapiro I L 1992 *Effective Action in Quantum Gravity* (Bristol: Institute of Physics Publishing)
- [19] Camporesi R 1990 *Phys. Rep.* **196** 1–134
- [20] Berger M 1968 *Rev. Roum. Math. Pures Appl.* **7** 915–31
- [21] DeWitt B S 1975 *Phys. Rep.* **19** 295–357
- [22] Fisher M P A and Fradkin E 1985 *Nucl. Phys. B* **251** 457–71
Ludwig A W W, Fisher M P A, Shankar R and Grinstein G 1994 *Phys. Rev. B* **50** 7526–52
Mudry C, Chamon C and Wen X G 1996 *Nucl. Phys. B* **466** 383–443
Furusaki A 1999 *Phys. Rev. Lett.* **82** 604–7